Applied Catalysis B: Environmental 339 (2023) 123105

Contents lists available at ScienceDirect

Applied Catalysis B: Environmental

journal homepage: www.elsevier.com/locate/apcatb

Laboratory aging of a dual function material (DFM) washcoated monolith for varying ambient direct air capture of CO_2 and *in situ* catalytic conversion to CH_4

Monica Abdallah, Yuanchunyu (Iris) Lin, Robert Farrauto *

Earth and Environmental Engineering, Columbia University in the City of New York, 500 West 120th Street, New York, NY 10027, USA

ARTICLE INFO

Keywords:
CO_2 direct air capture
CO_2 methanation
Dual function material
Monolith
Ambient aging study

ABSTRACT

A DFM has been designed for direct air capture of CO_2 and *in situ* catalytic methanation for sustainable natural gas production. It is composed of 1% Ru, 10% "Na_2O"/γ-Al_2O_3//ceramic monolith, the latter with high open frontal area to reduce pressure drop when processing real air. Extended laboratory aging was conducted using simulated ambient capture conditions varying in temperature and humidity for over 100 cycles (450+ hours on stream). The continuous test protocol was designed to simulate some representative ambient conditions expected during advanced pilot plant testing. The capture step was followed by catalytic hydrogenation of CO_2 to methane during a temperature swing to 300°C. Results demonstrated stable, repeatable CO_2 capture and CH_4 production with no evidence of sorbent or catalyst deactivation. These findings support the case for further advanced testing to substantiate scale up of this material for producing a useful fuel or feedstock while mitigating climate change.

1. Introduction

1.1. Background

It is well understood that continued reliance on fossil fuels will further intensify the issue of rising atmospheric CO_2 concentrations and climate change [1]. Emission reductions, as well as removal and storage of atmospheric CO_2, are integral to limiting global warming [1,2]. In accordance with these goals, it is necessary to find sustainable ways of deriving critical carbon-based products from atmospheric CO_2 to meet the needs of commercial markets while reducing the demand on fossil fuels. In the United States, this shift has been emphasized by enhancements of 45Q tax credits for CO_2 capture and utilization, which are outlined in the Inflation Reduction Act of 2022 [3].

Many examples of CO_2 conversion through thermochemical, electrochemical, or biochemical means, for example, are exemplified in the literature, reinforcing potential pathways to a circular carbon model for producing fuels and chemicals [4–6]. CO_2 reduction products that have been studied include carbon monoxide, formic acid, methanol, methane, and light hydrocarbons [4,5]. While avenues to CO_2-derived products exist, sourcing CO_2 from the atmosphere through direct air capture (DAC) is a requisite step for carbon-neutrality and a circular carbon economy. However, DAC has intrinsic challenges. Capturing dilute atmospheric CO_2 (approximately 418 ppm) [7] is more energy intensive than capture from point sources and must use low-cost renewable energy to minimize cost and mitigate CO_2 emissions. Furthermore, the costs and emissions associated with concentration, pressurization, and transportation of CO_2 to the site of utilization must also be considered. The nature of DAC allows for freedom of location, enabling co-location with renewable electricity plants or near downstream processing infrastructure where the CO_2 conversion product can be further upgraded [4,8]. As expected, this is subject to sorbent limitations since ambient air varies in temperature and composition (i.e., humidity) depending on location, season, and time of day. In theory, intensifying the capture and catalytic conversion processes can offer major benefits, including eliminating the need for access to CO_2 pipelines or other storage and transportation infrastructure [9].

With the emergence of new sorbents and catalysts, it is now feasible to integrate CO_2 capture with *in situ* catalytic conversion to achieve this goal. A notable example of such a technology is the dual function material (DFM), which is typically composed of a CO_2 sorbent, often an alkali or alkaline earth oxide or carbonate, and conversion catalyst [10,11]. By dispersing these species on a high surface area carrier, the material exemplifies intrinsic capture and catalytic conversion properties,

* Corresponding author.
E-mail address: rf2182@columbia.edu (R. Farrauto).

https://doi.org/10.1016/j.apcatb.2023.123105
Received 10 May 2023; Received in revised form 14 July 2023; Accepted 16 July 2023
Available online 17 July 2023

enabling both processes to occur on the material's surface. Originally conceived for methane generation (synthetic or sustainable natural gas) [10,11], the DFM can be designed and applied to generate different chemicals and fuels, making it a platform for CO_2-derived products. For example, DFMs have been used to generate syngas through reverse water gas shift [12–15] and dry ethane reforming [16]. Still, methane generation by means of the Sabatier reaction is the most extensively studied and shows great promise for navigating the initial pathway to carbon-neutral fuels and a synthesis gas feedstock for Fischer-Tropsch processes.

Ru and Ni are most often used in DFMs for methane production due to their high activity and selectivity [10,11,17–34]. Associated CO_2 sorbents are composed of Na [11,17–28,35,36], Mg [11,18], K [11,12,18,27,37], Ca [10,18,23–26,29,34], Ba [30,37], and Li [27,31]. In these studies, the CO_2 source concentration varies from atmospheric levels (400+ ppm) to 15% or even higher, reflecting both DAC and point source applications. In particular, a DFM composed of "Na_2O" and Ru dispersed over γ-Al_2O_3 and has been studied extensively for capture and *in situ* methanation from simulated power plant flue gas (7.5% CO_2) [18,21,32–36]. Work by our group published in this journal has examined this material for combined direct air capture (DAC) and methanation, henceforth referred to as DACM [19,20]. A feasibility study adapted the DFM process from point source capture and methanation to DACM under isothermal conditions, where both capture and conversion occurred at 320°C, reflecting the previous embodiment [19]. A packed bed study showed the DFM was able to capture CO_2 from dilute sources of CO_2 and effectively convert it to CH_4. Ultimately, heating ambient air to achieve this isothermal process is impractical, so further studies evaluated the DFM for DACM in a temperature swing configuration, where capture was performed under simulated ambient conditions and methanation was performed at 300°C [20]. A packed bed study of 1% Ru, 10% Na_2O/Al_2O_3 DFM granules revealed good repeatability over 10 cycles of DACM under dry simulated ambient capture conditions. Further evaluations simulating humid capture demonstrated over three times greater CO_2 capture than in dry conditions and, correspondingly, more CH_4 generated, highlighting the positive impact of moisture that is present in the atmosphere for any DAC application [20]. A schematic of the integrated DACM process, utilizing a monolith support, is depicted in Fig. 1 and highlights how both capture and *in situ* conversion occur within one DFM reactor.

In this proposed process, the DFM is first exposed to ambient air, during which CO_2 selectively chemisorbs to capture sites. The O_2 present in air oxidizes the Ru catalyst, forming RuO_2. After CO_2 saturation, O_2 and unreacted CO_2 are removed via an inert purge or light vacuum. The material is then heated with a renewable energy source to approximately 200 °C in the presence of green H_2, during which RuO_2 is reduced to Ru^0 and made catalytically active for methanation via the Sabatier reaction. Upon complete methanation of captured CO_2, adsorption sites are available for reuse. In this way, the DFM can repeatedly capture CO_2 and convert it to CH_4—or sustainable natural gas if green H_2 is used—in a cyclic manner within a single reactor.

1.2. Surface mechanism for capture and in situ methanation of CO_2

The mechanism for CO_2 capture and conversion over the Ru, Na_2O/Al_2O_3 DFM was discussed by Proaño et al. following analysis via *in situ* DRIFTS under isothermal conditions at 320°C mimicking point source capture [33]. This study showed that CO_2 is adsorbed as a bidentate carbonate to $Al-O^- - Na^+$ species, highlighting a synergistic interaction between Na_2O and γ-Al_2O_3 that plays a role in CO_2 capture. During hydrogenation, DRIFTS spectra present intense formate peaks coincident with methane peaks and the disappearance of bidentate carbonate peaks, revealing formate as a key reaction intermediate. In this step, surface hydrides form due to dissociative adsorption of H_2 on Ru active sites. The authors propose that neighboring hydrides are added to the bidentate surface species, forming H_2O, followed by spillover of the adsorbate to a neighboring Ru metal site. Here, it combines further with dissociated H_2 to form CH_4. During CO_2 capture where O_2 is present (i.e., DAC), neither capture nor spillover occur on the Ru sites that are the oxidized state (RuO_2). Once the RuO_2 is reduced to metallic Ru during the hydrogenation step, the spillover and subsequent methanation can

Table 1
Simplified steps of CO_2 capture and conversion over the Ru+Na_2O DFM [33].

Step		Reaction	Temp (°C)	Relative rate	Notes
Adsorption	1	CO_2 + "Na_2O" ⟶ "Na_2O"···CO_2	Ambient	fast	CO_2 adsorbs to $Al-O^- - Na^+$ surface species
	2	Ru + O_2 ⟶ RuO_2			Ru is oxidized by O_2 in capture feed
Methanation	1	RuO_2 + 2 H_2 ⟶ Ru + 2 H_2O	150 °C [20]	fast	RuO_2 is reduced by green H_2
	2	"Na_2O"···CO_2 + Ru ⟶ "Na_2O" + Ru···CO_2	≥150 °C	slow	Adsorbed CO_2 spills over to Ru
	3	Ru···CO_2 + 4 H_2 ⟶ Ru + CH_4 + 2 H_2O	≥175 °C [20]	fast	Methanation proceeds over Ru

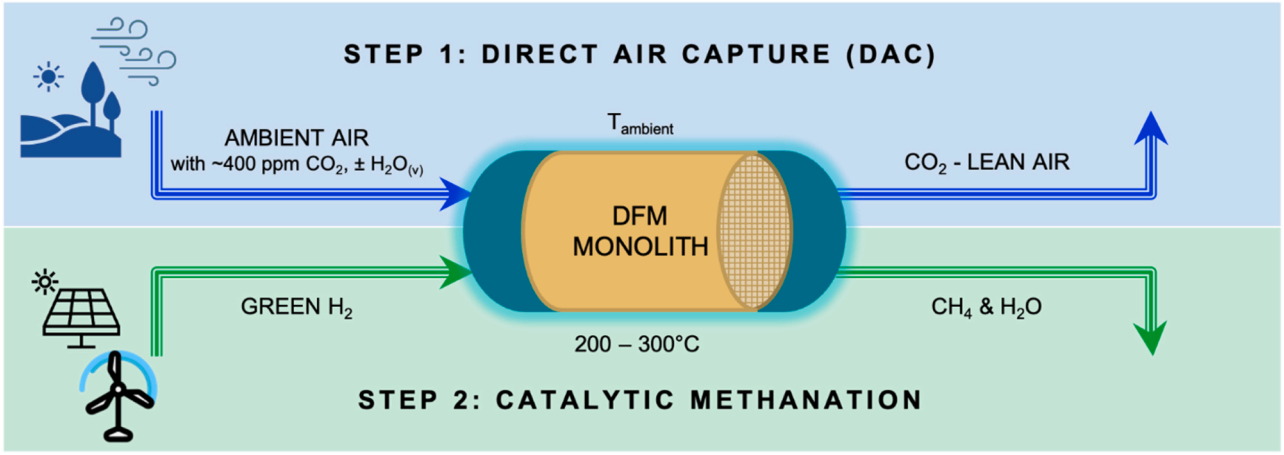

Fig. 1. Overview of integrated direct air capture and methanation (DACM) using a monolith-supported dual function material (DFM).

proceed. Simplified steps are shown in Table 1.

Additional studies by Jeong-Potter et al. show Ru facilitates a significant enhancement of capture capacity by catalytically decomposing surface carbonates during hydrogenation, which results in available sites for subsequent CO_2 capture [22]. Samples of "Na_2O"/Al_2O_3 with and without Ru were pre-treated in H_2 at 300 °C before cooling and a subsequent CO_2 capture step. The Ru-containing sample (DFM) captured nearly double the amount of CO_2 than the supported sorbent alone. These results were echoed in packed bed tests. DFM samples underwent several cycles of DAC and methanation, while the supported sorbent sample underwent capture and desorption in N_2 at the same temperatures (25 °C adsorption, 300 °C methanation or desorption). The DFM repeatedly captured more CO_2 than the supported sorbent, further highlighting the role of Ru in freeing capture sites through catalytic methanation. Higher Ru loadings corresponded to greater capture capacity and, correspondingly, greater methane production.

This capacity enhancement is yet another unique advantage of using the DFM for integrated capture and conversion and reinforces why co-dispersal of sorbent and catalyst is superior to physical mixture of the supported components, which was previously demonstrated by Duyar et al. for a Ru-based DFM containing CaO [10]. The nature of the interaction between adsorbed CO_2 and catalyst active sites was the subject of previous work where thermogravimetric analysis was used to investigate the kinetics of methanation by a Ru+Na_2O DFM at temperatures from 200 °C to 320 °C [38]. Kinetics studies are typically performed by co-feeding reactants under differential conditions, but in DFM applications, reactants are introduced separately, where the CO_2 is first adsorbed followed by the introduction of H_2 for methane production. The activation energy for methanation over the DFM was calculated to be half that of methanation over the supported Ru catalyst, resulting in the speculative conclusion that migration of adsorbed CO_2 to the active sites is somewhat limiting [38], and an additional publication by Wang et al. implicitly acknowledges the role of the spillover phenomenon in methanation [35].

1.3. Goals

As mentioned, previous packed bed studies demonstrated stability of a Ru+Na_2O DFM over 10 cycles of DACM and an overall performance enhancement when moisture (humidity) is present during simulated DAC [20]. Our current work seeks to evaluate long term stability of a DFM washcoated monolith under simulated varying ambient conditions. Significant volumes of ambient air must be processed to capture meaningful quantities of CO_2, which will lead to significant pressure drop, a notable reactor design challenge for DAC applications [39]. This issue echoes that of the automobile catalytic converter, where pressure drop due to the high velocity of exhaust gas required the use of monolithic catalyst supports with high open frontal areas to reduce pressure drop penalties on performance and energy costs [40,41]. Monoliths are also well known for their long-term mechanical and thermal stability and high geometric surface area.

The DFM is synthesized in the form of a washcoat deposited on the channel walls of a commercially available cordierite ceramic monolith. A monolith with an open frontal area approaching 90% for reduced pressure drop and high geometric surface area (600 cpsi) was chosen for increased washcoat loadings and, consequently, CO_2 capture capacities. Along with demonstrating the durability of a DFM-washcoated monolith, recent work has emphasized the evaluation of the DFM performance under several simulated DAC conditions that reflect potential capture climates. Naturally, ambient conditions vary widely with time of day, season, and location; thus, it is necessary to evaluate the performance of the sorbent-catalyst combination over time and in conditions that mimic the variability of the climates it may encounter [42]. Identifying and understanding changes in performance can provide valuable data for improving the material and, ultimately, determining the best locations or climates for deployment.

2. Experimental

2.1. Materials preparation

2.1.1. DFM washcoated monolith

An aqueous slurry composed of 35 wt% γ-Al_2O_3 powder (35 μm, Sasol) was ball milled for 6 h. A monolith (cordierite, 2 mil walls, 600 cells per square inch, 0.75″ dia. x 0.75″ len., NGK Insulators) was weighed before being dipped into the Al_2O_3 slurry. The channels were cleared of excess slurry with a concentrated stream of air. The Al_2O_3-washcoated monolith was dried (120 °C) and calcined (500 °C, 4 h) in air to ensure adhesion of the coating to the walls of the monolith. It was weighed and then loaded sequentially with precursor solutions of the catalyst and sorbent to fully synthesize the DFM washcoat. The target Ru loading (1 wt%) was achieved by incipient wetness impregnation whereby the monolith was dipped into an aqueous solution of 1.5 wt% $Ru(NO)(NO_3)_3$ (Alfa Aesar). The sample was dried (120 °C) and reduced in 20% H_2/N_2 at 300 °C for 8 h before room temperature passivation in 1 % O_2 to form an insoluble surface layer of RuO_x. The monolith was dipped into an aqueous solution of 6 wt% Na_2CO_3 (Sigma Aldrich) and dried overnight (120 °C). The fully coated monolith was again weighed to establish the total washcoat loading.

The completed DFM-washcoated monolith was pretreated in 20% H_2/N_2 at 300 °C (2 NL $h^{-1}g_{DFM}^{-1}$, 3 h) in the tubular reactor before commencing cyclic studies. The final DFM is about 1% Ru, 10% "Na_2O"/Al_2O_3//monolith, with a washcoat loading (WCL) of 1.4 g/in^3. The "Na_2O" is a designated term since the sodium species has no detectable structure (i.e. amorphous to XRD) [33].

2.1.2. Equivalent DFM granules for ease of characterization before and after 20 cycles of aging

DFM granules with the same composition as the washcoated DFM monolith (1% Ru, 10% "Na_2O"/γ-Al_2O_3) were included in the reactor immediately downstream from the DFM monolith. After multiple cycles, they were removed and characterized while the monolith was used for additional ambient condition testing. This allows for ease of partial characterization of aged materials.

DFM granules were synthesized via incipient wetness impregnation of precursor salts. An aqueous solution of 6.1 wt% $Ru(NO)(NO_3)_3$ (Alfa Aesar) was impregnated onto γ-Al_2O_3 granules (300 μm, Sasol). Once the target loading of Ru was achieved, the sample was dried (120 °C) and reduced in a flow of 20% H_2/N_2 at 300°C for 3 h. The reduced Ru was passivated in 1% O_2 at room temperature to form insoluble surface layer of RuO_x. An aqueous solution of 13.4 wt% Na_2CO_3 (Alfa Aesar) was adsorbed by the Ru-containing Al_2O_3 washcoat via incipient wetness and dried overnight (120°C). Once dried, the incipient wetness procedure was repeated with a solution of 12.8 wt% Na_2CO_3 to achieve the target concentration of 10 wt% "Na_2O." Once impregnation was complete, the sample was loaded into the reactor and reduced in 20% H_2/N_2 at 300 °C (2 NL $h^{-1}g_{DFM}^{-1}$, 3 h) before commencing cyclic studies.

2.2. Reactor studies

2.2.1. Reactor setup

All reactor studies were conducted by loading DFM samples into a quartz tube reactor (22/25.8 mm × 550 mm). Samples were secured with glass wool (Supelco Inc, USA). The monolith was wrapped in Fiberfrax to fit securely in the reactor. The remaining space in the reactor was packed with glass beads (McKesson, USA) to decrease dead volume. The reactor tube was fitted in a microthermal furnace (MTSC12.5 R x 18–1Z, Mellen, USA), and a K-type thermocouple (Omega, USA) resting at the inlet face of the monolith was used for temperature feedback control. Mass flow controllers (MKS Instruments) were used to feed and mix compressed gases at designated flow rates. Three-way valves are situated such that the process gas can be diverted into a water saturator at ambient temperature (approximately 25 °C),

producing humidity at approximately 2 mol% H_2O, or approximately 90% relative humidity (RH) at 25 °C. Alternatively, the process gas can bypass the saturator. An ice bath was placed at the exit of the reactor to condense moisture in the exhaust for precise analysis. The exit gas composition during the adsorption step was analyzed at NTP in a LI-830 CO_2 gas analyzer (LI-COR, USA) for ppm-level detection of CO_2 (± 2 ppm accuracy). During methanation, the reactor exhaust flow path is split for simultaneous analysis by two gas analyzers. The second analyzer used is an Enerac 700 (Enerac, USA) for ppm-level detection of CH_4 (5% accuracy for hydrocarbons). The general reactor configuration is shown in previous work [20].

2.2.2. Reactor operation

Table 2 shows the steps for integrated DAC and methanation, henceforth referred to as DACM. Each cycle begins with a CO_2 capture (adsorption) step at a specified temperature and humidity condition and proceeds until full CO_2 saturation is reached. The range of full capture durations for the various conditions tested is given in Table 2. The reactor is then purged with N_2 to evacuate the reactor of air, non-adsorbed CO_2, and humidity before proceeding with methanation. A flow of 15% H_2/N_2 is introduced, and the reactor is heated at approximately 10 °C/min to 300 °C, which is the maximum temperature envisioned for complete methanation of adsorbed CO_2. The reactor temperature is maintained at 300 °C until the effluent CH_4 concentration is less than 100 ppm, indicating the methanation step is essentially complete.

2.3. H_2 pulse chemisorption

Ruthenium dispersion of the fresh and aged DFM granule samples were determined via H_2 pulse titration (ChemBET Pulsar TPR/TPD, Quantachrome). Approximately 0.5 g of sample was used for analysis. Each sample was reduced *in situ* at 320°C for 3 h in 20% H_2/N_2 (30 ml/min). After reduction, a N_2 purge (30 ml/min) was initiated, and the sample temperature was reduced to 100°C for subsequent chemisorption analysis.

3. Results & discussion

3.1. Monolith validation and short-term stability — 25 °C + 2 mol% H_2O simulated capture condition

The performance of the 1% Ru, 10% "Na_2O"/Al_2O_3//monolith, henceforth referred to as the DFM monolith, was validated through multi-cycle DACM stability testing. In these tests, the adsorption temperature was 25 °C and moisture was added to the synthetic air feed (2 mol% H_2O, or 90% RH). In addition to evaluating CO_2 capture and CH_4 production, Ru dispersion changes were of interest. To avoid the need to scrape the DFM washcoat from the cordierite monolith or pulverize the monolith for characterization, granules with the same composition as the DFM monolith washcoat (see preparation in Section 2.1.2) were situated immediately downstream from the DFM monolith for both samples to be cycled under identical conditions. In doing so, the integrity of the DFM monolith could be maintained for further cyclic testing while a similarly prepared sample was exposed to the same experimental aging conditions. After cyclic capture and methanation (DACM cycles), the DFM granules were removed for further characterization while cyclic aging of the monolith was continued. A comparison of initial and final performance after 20 cycles of aging is shown in Fig. 2.

Table 2
Outline of DACM cyclic aging steps.

	Step	Temp. (°C)	Gaseous environment	Flow rate NL h^{-1} $g^{-1}_{washcoat}$	Duration
1	Adsorption	0, 25, or 40	400 ppm CO_2/air ± 2 mol% H_2O	48	1.5–4 h
2	Purge	0, 25, or 40	Pure N_2	12	20 min
3	Heating	~10 °C/min	15 % H_2/N_2	12	~30 min
4	Methanation	T_{max} = 300	15 % H_2/N_2	12	0.5–1 h

The fresh DFM monolith captured an average of 1058 ± 20 μmol $CO_2/g_{washcoat}$ and produced an average of 563 ± 39 μmol $CH_4/g_{washcoat}$ per cycle, corresponding to an average total CO_2 conversion of 53%. After 20 cycles, the conversion increases to 58%. While a slight improvement in capture capacity is observed, this increase was not observed in subsequent cyclic tests. Given the relative consistency of the data, the DFM monolith was validated as a good candidate for further examination.

Fig. 3 shows the reactor temperature and effluent concentrations of CO_2 and CH_4 during the heating and methanation steps under 15% H_2/N_2 flow. The data show CO_2 desorption over a range of temperatures, and a maximum CO_2 concentration is reached between 150 °C and 160 °C. RuO_2 is reduced to catalytically active Ru^0 at approximately 150 °C [20], and methanation is initiated at about 200 °C (Fig. 3). At this point, the concentration of unreacted CO_2 in the effluent decreases significantly and eventually diminishes as methanation dominates. It is believed that a large extent of the desorption observed herein is an artifact of slow heating (10 °C/min) and the 15% H_2/N_2 used in the laboratory due to safety considerations. It is expected that at scale, rapid, efficient washcoat heating and 100% green H_2, which will likely be pressurized in a commercial unit, will accelerate methanation kinetics, decreasing the light-off temperature and increasing the yield of CH_4 produced.

3.2. DFM characterization

DFM granules (1% Ru, 10% "Na_2O"/Al_2O_3) were placed downstream from the DFM monolith and cycled 20 times (Section 3.1). Results of H_2 chemisorption studies on fresh and "aged" DFM granule samples are shown in Table 3. The dispersion decreased from its fresh state of 11.98% to 7.31% after 20 cycles of DACM, which is indictive of some sintering. The instrument calculation shows the growth in average crystallite size from 111 Å to 182 Å after 20 cycles of DACM. Although it appears sintering has occurred, the data in Fig. 2 show that the average

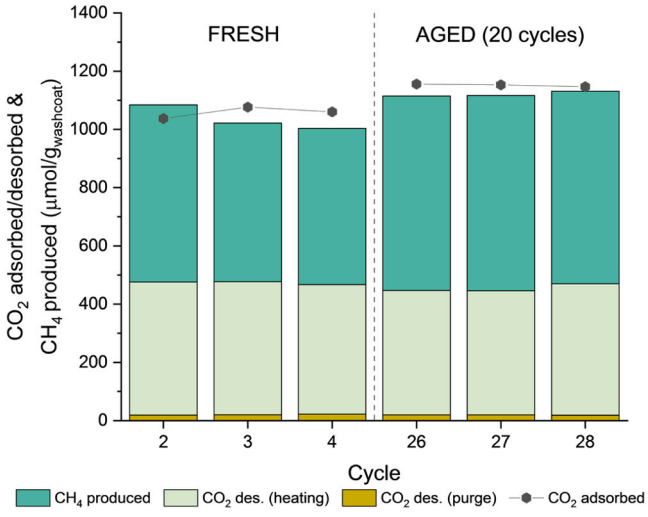

Fig. 2. Comparison of fresh and 20 cycle "aged" performance of 1% Ru, 10% "Na_2O"/Al_2O_3//monolith. WCL = 1.4 g/in^3. Cycles consist of adsorption to full capture capacity (25 °C, 400 ppm CO_2/air + 2% H_2O, 4 h) followed by heating & methanation (10 °C/min to 300 °C, 15% H_2/N_2, 1.5 h hold).

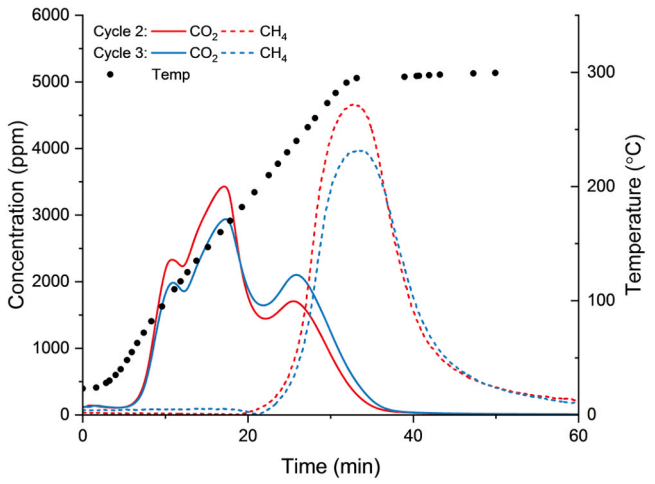

Fig. 3. Effluent CO_2 desorption and CH_4 generation signals from the DFM monolith (1% Ru, 10% "Na_2O"/Al_2O_3//monolith, WCL = 1.4 g/in^3) reactor during heating and methanation (10 °C/min to 300 °C) in 15% H_2/N_2.

Table 3
Ru dispersion of 1% Ru, 10% "Na_2O"/Al_2O_3 DFM granules.

Sample	Ru dispersion (%)	Calculated avg. crystallite size (Å)
Fresh DFM granules	11.98	111.34
20 cycle "aged" DFM granules	7.31	182.41

quantity of CH_4 produced remains stable.

Previous DFM characterization via H_2 chemisorption and TEM-EDS demonstrated a redispersion of aged Ru in Ru-only and Ru+Ni combination DFMs for flue gas (point source) applications at 320 °C [17,36]. However, redispersion of Ru in DFM samples with relatively lower loadings of Ru for the ambient DACM application has not been observed to date, as shown here and in previous work [20]. X-ray diffraction (XRD) has confirmed the formation of RuO_2 during exposure to air and the presence of metallic Ru after hydrogenation [36]. XRD patterns do not indicate the presence of crystalline Na species, confirming that the alkaline sorbent is amorphous. The stability of the "Na_2O" sorbent dispersion is demonstrated herein through consistent isothermal CO_2 chemisorption behavior over 20+ cycles. Similarly, the Ru dispersions show evidence of some sintering but does not affect the methanation performance. DFM performance stability was the subject of further examination under various simulated DAC conditions, and data presented in Fig. 2 were used as a baseline reference for comparing performance during and after aging.

3.3. Extended laboratory aging of the DFM monolith in various simulated ambient adsorption conditions

The positive findings following 20+ cycles of DACM (Fig. 2) encouraged further study of the 1% Ru, 10% "Na_2O"/Al_2O_3//monolith under varying simulated ambient capture conditions. Given that ambient air conditions vary greatly depending on location, season, and time of day, it is necessary to establish a test protocol to evaluate the stability of CO_2 capture performance under continuous changes in the ambient conditions.

The quantities of CO_2 captured and CH_4 generated were measured during DACM cycles where capture conditions varied as presented in Fig. 4. The adsorption condition previously evaluated (25 °C with humidity, or 2 mol% H_2O) was chosen as a reference condition (yellow star) for evaluating comparative changes in performance over time. After performance testing at the specified simulated capture conditions (i.e., 0 °C, 40 °C), additional cycles were carried out at the reference condition to establish whether changes in performance occurred. Time on stream (TOS) spent at each experimental condition is included. TOS is calculated as the summation of hours spent during the capture (oxidizing environment) and methanation steps (reducing environment) over all cycles.

3.3.1. DFM monolith performance at 40 °C + 2 mol% H_2O capture condition

Continuous cycles of DACM were conducted using an elevated CO_2 capture temperature, 40 °C with 2 mol% H_2O (28% RH), reflecting a hot climate with mild humidity (Table 2). The methanation conditions were kept constant. The results of the multi-cycle tests are shown in Fig. 5. The hatched bar labeled 'A′ shows the performance of the fresh DFM monolith at the reference condition (25 °C, 2 mol% H_2O), while the hatched bar labeled 'B′ is the performance at the reference condition after aging at 40 °C. The consistency here shows the adaptability of the DFM, as the data show no decline in either CO_2 capture or CH_4 produced after the excursion to 40 °C.

The first several cycles at 40 °C show an equilibration period before reaching stability in overall CO_2 adsorption. The average CO_2

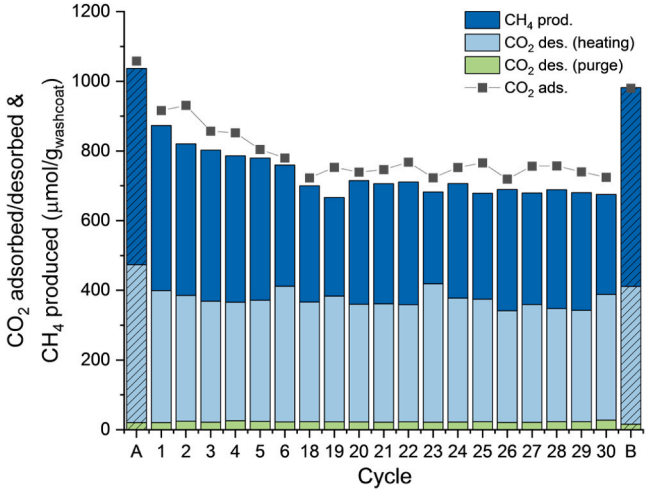

Fig. 5. Cumulative CO_2 adsorbed/desorbed & CH_4 produced during cyclic DACM on 1% Ru, 10% "Na_2O"/Al_2O_3//monolith. WCL = 1.4 g/in^3. Cycles consist of adsorption (40 °C, 400 ppm CO_2/air + 2 mol% H_2O, 3 h hold) followed by heating & methanation (~10 °C/min, 300 °C, 15% H_2/N_2, 0.5 h). Hatched bar 'A′ represents fresh DFM monolith performance at 25 °C and 2 mol % H_2O (reference) for comparison. Hatched bar 'B′ gives DFM monolith performance at the reference condition obtained after the conclusion of DACM cycles using 40 °C adsorption temperature.

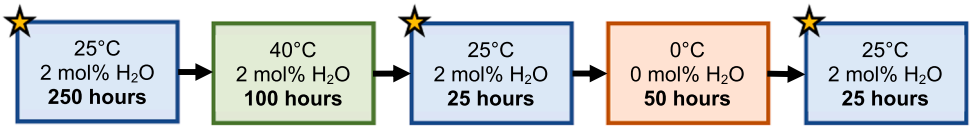

Fig. 4. Experimental overview of simulated DAC conditions during multi-cycle DACM testing of DFM monolith. Heating rate (10 °C/min) up to the target temperature (300 °C) and gaseous environment (15 % H_2/N_2) were kept constant during subsequent methanation steps (not depicted).

adsorption in the last 10 cycles is 745 ± 18 μmol/$g_{washcoat}$ at 40 °C is roughly 35% lower than the reference case (25 °C and 2 mol% H_2O), given by the hatched bar labeled 'A′ in Fig. 5. Given that adsorption is exothermic and less thermodynamically favorable at higher temperatures, it was expected that the capture capacity would be lower than at the reference temperature. Nonetheless, it was found that at this higher temperature capture condition the DFM still remains stable for integrated DACM and demonstrates repeatable behavior, though at a reduced level of CO_2 capture and CH_4 production. It should be noted from cycles 7 – 17, a laboratory upset occurred, so the data were omitted from this analysis and additional cycles, with the same DFM material, were performed to ensure material stability under these conditions. However, the consistency between cycles 5/6 and 18+ show stable performance in both CO_2 captured and CH_4 produced. The upset condition obviously had no impact on the DFM function, showing system reliance.

3.3.2. *DFM monolith performance at 0 °C + 0 mol% H_2O capture condition*

Multi-cycle testing was performed at 0 °C in the absence of moisture to simulate a dry, wintry climate (Fig. 6). This test continued the sequence of continuous evaluation as shown in Fig. 4. The hatched bar labeled 'A′ shows the performance of the fresh DFM monolith at the reference condition (25 °C, 2 mol% H_2O), while the hatched bar labeled 'B′ is the performance at the reference condition after aging at 0 °C. The CO_2 capture temperature was designed to be close to 0 °C by using a cold pack at -20 °C. Therefore, during these tests, the temperature fluctuated from -10°C to 10°C, causing scatter in the adsorption data. There is an initial equilibration period, as was previously evident in the 40 °C cycles (Fig. 5), after which the DFM monolith shows regular repeatable quantities of CO_2 adsorbed and CH_4 generated. After 15 cycles at the 0 °C capture condition with no added moisture, the average quantity CO_2 captured was 368 ± 45 μmol/$g_{washcoat}$ and the average quantity of CH_4 produced was 153 ± 9 μmol/$g_{washcoat}$. It is important to note that moisture was absent during 0 °C studies to avoid the formation of ice. The decrease in CO_2 adsorption has been attributed to the absence of humidity, which we reported to enhance CO_2 adsorption [20]. Regardless, the results show that when the adsorption conditions are adjusted to the reference condition (B), stable performance is achieved once again.

3.3.3. *Summary of aging under various DAC conditions*

A comparison of continuous DFM monolith performance is given in Fig. 7. From left to right, the stacked bars indicate averaged CO_2 capture, CO_2 desorption, and CH_4 generation corresponding to various simulated ambient capture conditions that were evaluated, as outlined in Fig. 4. The stars indicate the average DACM performance at the reference capture condition (25 °C, 2 mol% H_2O), which was re-evaluated regularly throughout the study and shows the DFM monolith captures CO_2 consistently over time with no signs of deactivation. Within each test condition, the CO_2 capacity and CH_4 production stabilizes, demonstrating repeatable performance and the ability of the DFM to adapt as the climate conditions fluctuate. This is a critical finding for it further confirms the potential for reliability of the DFM. Naturally, this must be confirmed in real pilot plant testing.

The absence of major deactivation is also supported by the normalized CH_4 generation data given in Fig. 8, which shows consistency in light off temperature after 100 DACM cycles under varying simulated ambient conditions. The slope of this line can be interpreted as the apparent rate of CH_4 generation. This further supports the finding that despite sintering of Ru (observed in the chemisorption data in Table 2), there is no hinderance in methanation capability of the DFM. Consistent with previous findings that indicated spillover as the rate limiting step, this data suggests that methanation is not kinetically controlling the rate and that reductions in catalyst loading may be possible without sacrificing performance.

3.4. *Additional considerations*

Optimizing conversion of CO_2 to CH_4 is an important area of concern for any process integrating DAC and conversion. As shown in Figs. 3 and 7, a consistent but significant amount of CO_2 is unreacted through desorption during heating from ambient conditions to the initiation of methanation. As previously mentioned, only 15% H_2/N_2 was used in these studies due to laboratory safety requirements. Pressurized, 100%

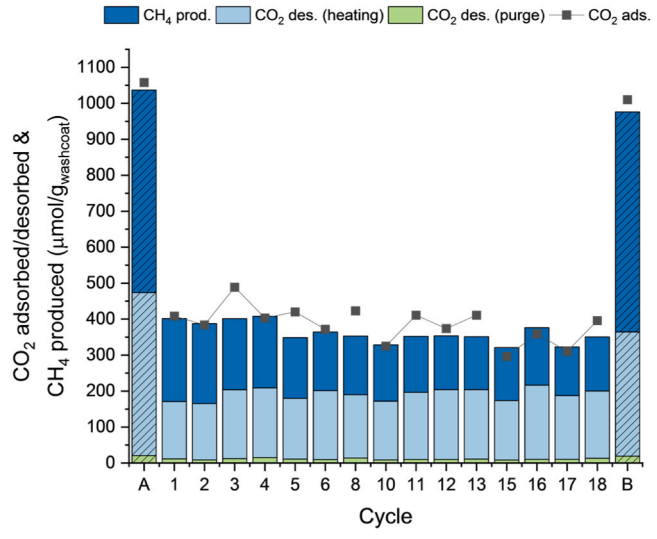

Fig. 6. Cumulative CO_2 adsorbed/desorbed & CH_4 produced over 15 cycles of DACM on 1% Ru, 10% "Na_2O"/Al_2O_3//monolith. WCL = 1.4 g/in^3. Cycles consist of dry adsorption (0 °C, 400 ppm CO_2/air, 1.5 h) followed by heating & methanation (~10 °C/min, 300 °C, 15% H_2/N_2, 0.5 h hold). Cycles 7, 9, and 14 are omitted due to a reactor leak. Hatched bar 'A′ gives average fresh DFM monolith performance generated at 25 °C and 2 mol% H_2O (reference) for comparison. Hatched bar 'B′ gives average DFM monolith performance at the reference condition after the conclusion of 0 °C adsorption tests.

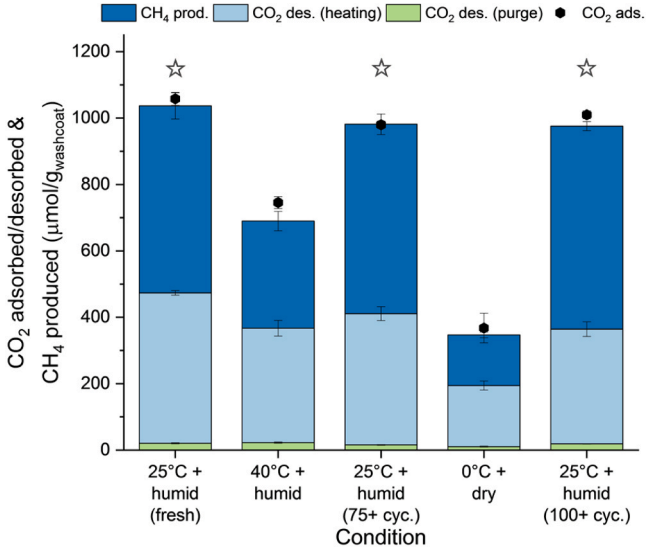

Fig. 7. Aging performance of DFM monolith over time and at various simulated DAC conditions. Data reflects the average performance during the last 10 DACM cycles at each adsorption condition indicated on the x-axis. If less than 10 cycles were performed, the calculated average is based on all cycles except the first. Adsorption conditions were varied as indicated, while heating & methanation remained constant (300 °C, 15% H_2/N_2). Error bars indicate the standard deviation of the sample.

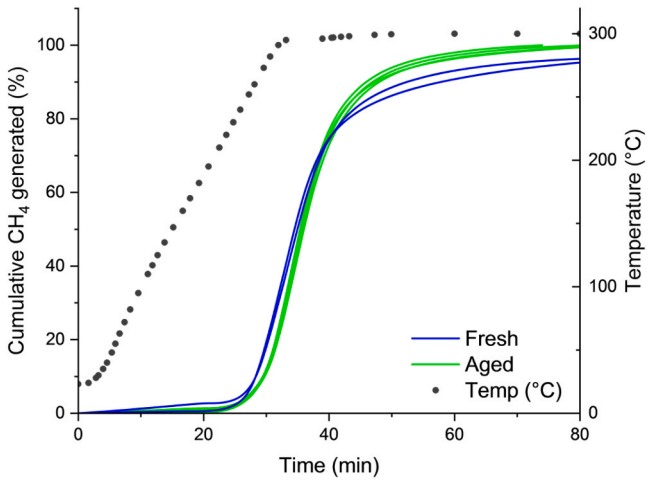

Fig. 8. Cumulative CH_4 generated (normalized) for fresh (blue, cycles 2 & 3) and aged (green, cycles 101–104) DFM monolith during the first 80 min of the methanation step.

green H_2 would be used in the field unit, which is expected to decrease the amount of unreacted CO_2 by accelerating methanation kinetics. A polishing catalyst can also be implemented downstream to remove smaller amounts of unreacted CO_2. Isolating the polishing catalyst from O_2 in the process design would allow for cheaper Ni to be used, which would mitigate the cost of this centralized unit for processing methanation effluent from all DFM reactors. Membrane separation can also be used to ensure the purity of CH_4 to be introduced to the existing pipeline infrastructure. It is expected that these will be addressed during engineering scale up.

Additional experiments were performed to better understand the nature of CO_2 desorption during heat up. The range of temperatures at which CO_2 desorption occurred (Fig. 3), as well as our previous work [20] and other examinations of alkaline sorbents [24,25,43], indicate that sorbent sites vary in basicity and strength. It is understood that weaker capture sites desorb CO_2 at lower temperatures, while stronger sites retain CO_2 until relatively higher temperatures are reached. Correspondingly, it has been found that the stronger surface carbonates form rapidly, followed by the slow formation of relatively weaker carbonates later in the adsorption step, which can easily desorb [37]. This phenomenon is reflected in cumulative adsorption profile (Fig. 9a), which exhibits a rapid rate of CO_2 uptake at the initiation of adsorption followed by a decrease in the rate of CO_2 uptake over time. In a separate study, the duration of the simulated DAC step was shortened to durations of 15, 50, and 90 min, which correspond to 20%, 50%, and 70% of total CO_2 capture capacity, respectively (Fig. 9a, Table 4). DACM cycles carried out at each partial capacity condition (% of maximum capacity, Table 4) reveal that the quantity of unreacted (desorbed) CO_2 is lowest in the 20% case. As the partial capacity increases, weakly adsorbed CO_2 begins to form and, correspondingly, the quantity of desorbed CO_2 increases (Fig. 9b). This is consistent with findings that stronger capture sites adsorb CO_2 first, followed by sites of decreasing strength, which is further reflected in the reduction in slope of the cumulative adsorption profile in Fig. 9a. Under the conditions tested, the strong CO_2 sites leveraged through short adsorption durations exhibit better retention during temperature swing and are likely to be converted to CH_4, which maximizes the use of captured CO_2.

These partial cycles reveal that the mode of operation can affect how efficiently CH_4 is produced. By calculating the average rate of CH_4 generation during a given DACM cycle (Table 4), a maximum production efficiency emerges when the DFM monolith is cycled at 50% adsorption capacity, where the DFM is 2.5x more productive than when cycled at full capture capacity (hatched bar, Fig. 9). During 50% capacity tests, the DFM produces 70% of the maximum potential CH_4, while "producing" 82% less unreacted CO_2. During 20% tests, practically no CO_2 desorbed during the temperature swing, but additional capture and conversion capacity are not utilized at this condition. Ultimately, DFM performance measured after implementing more advanced monolith heating methods and higher H_2 partial pressure during heating and methanation will better represent the capabilities of the DFM. Regardless, this experiment shows that designing cyclic modes to engage the most rapid adsorption kinetics and strongest capture sites can ensure the highest productivity during DACM operation.

4. Conclusion

A DFM comprising 1% Ru, 10% "Na_2O"/γ-Al_2O_3 was adapted to a washcoated monolith as a prototype design for pilot testing of direct air capture of CO_2 with subsequent catalytic conversion to CH_4. The extent of CO_2 capture and CH_4 production was shown to be stable throughout over 100 cycles or 450 h on stream during a cyclic aging study including various simulated ambient capture conditions. The extent of CO_2 capture and CH_4 produced varied for each ambient condition but always achieved stability within that condition. Overall, the system showed stable CO_2 capture and catalytic conversion at the reference test condition throughout 450 h under this testing protocol. Additional cyclic studies using partial capture capacity revealed the use of captured CO_2 was improved by leveraging strong CO_2 capture sites early in the

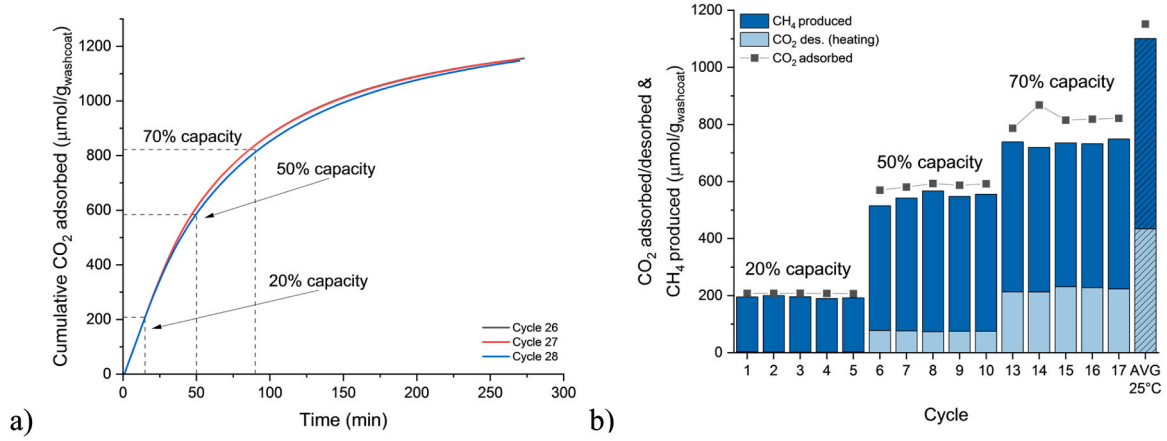

Fig. 9. (a) Cumulative CO_2 adsorbed by 1% Ru, 10% Na_2O/Al_2O_3//monolith (cordierite) during DAC step. WCL = 1.4 g/in^3. TOS > 200 h. (b) Partial capacity DACM cycles on DFM monolith. Hatched bar gives performance baseline generated at 25 °C and 90 % RH for comparison (TOS > 200 h). Cycles consist of adsorption (25 °C, 400 ppm CO_2/air + 2 mol% H_2O, 90% RH) followed by heating & methanation (300 °C, 15% H_2/N_2).

Table 4
Key parameters and performance metrics of partial capacity study.

Capacity % of max.	DAC duration min	Cycle duration* h	CO_2 adsorbed μmol $g^{-1}_{washcoat}$	CO_2 unreacted μmol $g^{-1}_{washcoat}$	CH_4 produced μmol $g^{-1}_{washcoat}$	Conversion %	CH_4 generation μmol $g^{-1}_{washcoat}$ h^{-1}
20	15	1.25	208	2	192	93	154
50	50	1.8	584	76	470	80	256
70	90	2.5	822	222	513	63	205
100	270	6.5	1152	434	667	58	102

Adsorption was performed with 400 ppm CO_2/air + 90 % RH at a flow rate of 48 NL h^{-1} g^{-1}. Data is given as the average of 5 cycles performed at each partial capacity condition.
* Includes adsorption, heating, and methanation. Excludes purge.

adsorption step. A maximum CH_4 production efficiency, calculated as CH_4 generated over time, was observed, underscoring an alternative method of evaluating CH_4 production. Furthermore, the washcoated monolith design in this study serves to address the critical pressure drop issue in DAC applications; at scale, this can mean a cost-effective way to achieve high throughput of air and contact between CO_2 and the DFM sorbent. The laboratory results highlight the technical merit of the DFM monolith and substantiate the case for bench testing and, ultimately, pilot testing of the DFM for intensifying CO_2 capture and catalytic conversion. Naturally, laboratory simulated conditions are only used as guidance for future testing in real ambient capture conditions. This will be the subject of pilot plant testing in the future.

CRediT authorship contribution statement

Monica Abdallah – Conceptualization, Methodology, Validation, Formal analysis, Investigation, Visualization, Writing – original draft. **Iris Lin** – Validation. **Robert Farrauto** – Conceptualization, Resources, Writing – review & editing, Supervision, Project administration, Funding acquisition.

Declaration of Competing Interest

The authors declare the following financial interests/personal relationships which may be considered as potential competing interests: Monica Abdallah and Iris Lin reports financial support was provided by Department of Energy (SBIR). None reports a relationship with None that includes:. None has patent None pending to None. None.

Data Availability

Data will be made available on request.

Acknowledgments

The authors would like to acknowledge the Department of Energy for their support of this work and scale up efforts through the United States Department of Energy (DOE) SBIR grant award no. DE-SC0020795 and our engineering partner, Susteon, Inc. Thank you to NGK Insulators, Sasol, and Anglo American for providing materials and insight. Thank you also to Dr. Michel Deeba and Wenhao Yan. The authors are also grateful to Ms. Viveka Gould and the J.G. Cohn Memorial Fellowship for many years of supporting research in environmental catalysis.

References

[1] Climate Change, The Physical Science Basis. Contribution of Working Group I to the Sixth Assessment Report of the Intergovernmental Panel on Climate Change, Cambridge University Press,, Cambridge, UK and New York, NY, USA, 2021, p. 2021.
[2] Climate Change, Impacts, Adaptation and Vulnerability. Working Group II Contribution to the Sixth Assessment Report of the Intergovernmental Panel on Climate Change, Cambridge University Press,, Cambridge, UK and New York, NY, USA, 2022, p. 2022.
[3] J. Yarmuth A., Inflation Reduction Act of 2022, 2022.
[4] R.G. Grim, Z. Huang, M.T. Guarnieri, J.R. Ferrell, L. Tao, J.A. Schaidle, Transforming the carbon economy: challenges and opportunities in the convergence of low-cost electricity and reductive CO_2 utilization, Energy Environ. Sci. 13 (2020) 472–494, https://doi.org/10.1039/C9EE02410G.
[5] Z. Huang, R.G. Grim, J.A. Schaidle, L. Tao, The economic outlook for converting CO_2 and electrons to molecules, Energy Environ. Sci. 14 (2021) 3664–3678, https://doi.org/10.1039/D0EE03525D.
[6] A. Saravanan, P. Senthil kumar, D.-V.N. Vo, S. Jeevanantham, V. Bhuvaneswari, V. Anantha Narayanan, P.R. Yaashikaa, S. Swetha, B. Reshma, A comprehensive review on different approaches for CO_2 utilization and conversion pathways, Chem. Eng. Sci. 236 (2021), 116515, https://doi.org/10.1016/j.ces.2021.116515.
[7] Global Monitoring Laboratory, Trends in Atmospheric Carbon Dioxide, National Oceanic and Atmospheric Administration. (2023). https://gml.noaa.gov/ccgg/trends/global.html (accessed February 1, 2023).
[8] A. Kätelhön, R. Meys, S. Deutz, S. Suh, A. Bardow, Climate change mitigation potential of carbon capture and utilization in the chemical industry, Proc. Natl. Acad. Sci. 116 (2019) 11187–11194, https://doi.org/10.1073/pnas.1821029116.
[9] P. Styring, H. de Coninck, H. Reith, K. Armstrong, Carbon capture and utilisation in the green economy: Using CO_2 to manufacture fuel, chemicals and materials, The Centre for Low Carbon Futures, 2011.
[10] M.S. Duyar, M.A.A. Treviño, R.J. Farrauto, Dual function materials for CO_2 capture and conversion using renewable H2, Appl. Catal. B: Environ. 168–169 (2015) 370–376, https://doi.org/10.1016/j.apcatb.2014.12.025.
[11] M.S. Duyar, S. Wang, M.A. Arellano-Treviño, R.J. Farrauto, CO_2 utilization with a novel dual function material (DFM) for capture and catalytic conversion to synthetic natural gas: an update, J. CO_2 Util. 15 (2016) 65–71, https://doi.org/10.1016/j.jcou.2016.05.003.
[12] L.F. Bobadilla, J.M. Riesco-García, G. Penelás-Pérez, A. Urakawa, Enabling continuous capture and catalytic conversion of flue gas CO_2 to syngas in one process, J. CO_2 Util. 14 (2016) 106–111, https://doi.org/10.1016/j.jcou.2016.04.003.
[13] H. Sun, J. Wang, J. Zhao, B. Shen, J. Shi, J. Huang, C. Wu, Dual functional catalytic materials of Ni over Ce-modified CaO sorbents for integrated CO_2 capture and conversion, Appl. Catal. B: Environ. 244 (2019) 63–75, https://doi.org/10.1016/j.apcatb.2018.11.040.
[14] G. Wang, Y. Guo, J. Yu, F. Liu, J. Sun, X. Wang, T. Wang, C. Zhao, Ni-CaO dual function materials prepared by different synthetic modes for integrated CO_2 capture and conversion, Chem. Eng. J. 428 (2022), 132110, https://doi.org/10.1016/j.cej.2021.132110.
[15] S. Sun, C. Zhang, S. Guan, S. Xu, P.T. Williams, C. Wu, Ni/support-CaO bifunctional combined materials for integrated CO_2 capture and reverse water-gas shift reaction: influence of different supports, Sep. Purif. Technol. 298 (2022), 121604, https://doi.org/10.1016/j.seppur.2022.121604.
[16] A. Al-Mamoori, A.A. Rownaghi, F. Rezaei, Combined capture and utilization of CO_2 for syngas production over dual-function materials, ACS Sustain. Chem. Eng. 6 (2018) 13551–13561, https://doi.org/10.1021/acssuschemeng.8b03769.
[17] M.A. Arellano-Treviño, N. Kanani, C.W. Jeong-Potter, R.J. Farrauto, Bimetallic catalysts for CO_2 capture and hydrogenation at simulated flue gas conditions, Chem. Eng. J. 375 (2019), 121953, https://doi.org/10.1016/j.cej.2019.121953.
[18] M.A. Arellano-Treviño, Z. He, M.C. Libby, R.J. Farrauto, Catalysts and adsorbents for CO_2 capture and conversion with dual function materials: limitations of Ni-containing DFMs for flue gas applications, J. CO_2 Util. 31 (2019) 143–151, https://doi.org/10.1016/j.jcou.2019.03.009.
[19] C. Jeong-Potter, R. Farrauto, Feasibility study of combining direct air capture of CO_2 and methanation at isothermal conditions with dual function materials, Appl. Catal. B: Environ. 282 (2021), 119416, https://doi.org/10.1016/j.apcatb.2020.119416.
[20] C. Jeong-Potter, M. Abdallah, C. Sanderson, M. Goldman, R. Gupta, R. Farrauto, Dual function materials (Ru+Na2O/Al2O3) for direct air capture of CO_2 and in situ catalytic methanation: the impact of realistic ambient conditions, Appl. Catal. B: Environ. (2021), 120990, https://doi.org/10.1016/j.apcatb.2021.120990.
[21] C. Jeong-Potter, A. Porta, R. Matarrese, C.G. Visconti, L. Lietti, R. Farrauto, Aging study of low Ru loading dual function materials (DFM) for combined power plant effluent CO_2 capture and methanation, Appl. Catal. B: Environ. 310 (2022), 121294, https://doi.org/10.1016/j.apcatb.2022.121294.
[22] C. Jeong-Potter, M. Abdallah, S. Kota, R. Farrauto, Enhancing the CO_2 adsorption capacity of γ-Al2O3 supported alkali and alkaline-earth metals: impacts of dual function material (DFM) preparation methods, Ind. Eng. Chem. Res. (2022), https://doi.org/10.1021/acs.iecr.2c00364.

[23] A. Bermejo-López, B. Pereda-Ayo, J.A. González-Marcos, J.R. González-Velasco, Mechanism of the CO_2 storage and in situ hydrogenation to CH4. Temperature and adsorbent loading effects over Ru-CaO/Al2O3 and Ru-Na2CO3/Al2O3 catalysts, Appl. Catal. B: Environ. 256 (2019), 117845, https://doi.org/10.1016/j.apcatb.2019.117845.

[24] A. Bermejo-López, B. Pereda-Ayo, J.A. Onrubia-Calvo, J.A. González-Marcos, J. R. González-Velasco, Aging studies on dual function materials Ru/Ni-Na/Ca-Al2O3 for CO_2 adsorption and hydrogenation to CH4, J. Environ. Chem. Eng. 10 (2022), 107951, https://doi.org/10.1016/j.jece.2022.107951.

[25] A. Bermejo-López, B. Pereda-Ayo, J.A. Onrubia-Calvo, J.A. González-Marcos, J. R. González-Velasco, Tuning basicity of dual function materials widens operation temperature window for efficient CO_2 adsorption and hydrogenation to CH4, J. CO_2 Util. 58 (2022), 101922, https://doi.org/10.1016/j.jcou.2022.101922.

[26] A. Bermejo-López, B. Pereda-Ayo, J.A. Onrubia-Calvo, J.A. González-Marcos, J. R. González-Velasco, Boosting dual function material Ni-Na/Al2O3 in the CO_2 adsorption and hydrogenation to CH4: joint presence of Na/Ca and Ru incorporation, J. Environ. Chem. Eng. 11 (2023), 109401, https://doi.org/10.1016/j.jece.2023.109401.

[27] S. Cimino, F. Boccia, L. Lisi, Effect of alkali promoters (Li, Na, K) on the performance of Ru/Al2O3 catalysts for CO_2 capture and hydrogenation to methane, J. CO_2 Util. 37 (2020) 195–203, https://doi.org/10.1016/j.jcou.2019.12.010.

[28] S. Cimino, E.M. Cepollaro, L. Lisi, Sulfur tolerance and self-regeneration mechanism of Na-Ru/Al2O3 dual function material during the cyclic CO_2 capture and catalytic methanation, Appl. Catal. B: Environ. 317 (2022), 121705, https://doi.org/10.1016/j.apcatb.2022.121705.

[29] H. Sun, Y. Zhang, C. Wang, M.A. Isaacs, A.I. Osman, Y. Wang, D. Rooney, Y. Wang, Z. Yan, C.M.A. Parlett, F. Wang, C. Wu, Integrated carbon capture and utilization: synergistic catalysis between highly dispersed Ni clusters and ceria oxygen vacancies, Chem. Eng. J. 437 (2022), 135394, https://doi.org/10.1016/j.cej.2022.135394.

[30] A. Porta, C.G. Visconti, L. Castoldi, R. Matarrese, C. Jeong-Potter, R. Farrauto, L. Lietti, Ru-Ba synergistic effect in dual functioning materials for cyclic CO_2 capture and methanation, Appl. Catal. B: Environ. 283 (2021), 119654, https://doi.org/10.1016/j.apcatb.2020.119654.

[31] S. Cimino, R. Russo, L. Lisi, Insights into the cyclic CO_2 capture and catalytic methanation over highly performing Li-Ru/Al2O3 dual function materials, Chem. Eng. J. 428 (2022), 131275, https://doi.org/10.1016/j.cej.2021.131275.

[32] L. Proaño, M.A. Arellano-Treviño, R.J. Farrauto, M. Figueredo, C. Jeong-Potter, M. Cobo, Mechanistic assessment of dual function materials, composed of Ru-Ni, Na2O/Al2O3 and Pt-Ni, Na2O/Al2O3, for CO_2 capture and methanation by in-situ DRIFTS, Appl. Surf. Sci. 533 (2020), 147469, https://doi.org/10.1016/j.apsusc.2020.147469.

[33] L. Proaño, E. Tello, M.A. Arellano-Trevino, S. Wang, R.J. Farrauto, M. Cobo, In-situ DRIFTS study of two-step CO_2 capture and catalytic methanation over Ru,"Na2O"/Al2O3 dual functional material, Appl. Surf. Sci. 479 (2019) 25–30, https://doi.org/10.1016/j.apsusc.2019.01.281.

[34] Q. Zheng, R. Farrauto, A. Chau Nguyen, Adsorption and methanation of flue gas CO_2 with dual functional catalytic materials: a parametric study, Ind. Eng. Chem. Res. 55 (2016) 6768–6776, https://doi.org/10.1021/acs.iecr.6b01275.

[35] S. Wang, E.T. Schrunk, H. Mahajan, A.R.J. Farrauto, The role of ruthenium in CO_2 capture and catalytic conversion to fuel by dual function materials (DFM), Catalysts 7 (2017), https://doi.org/10.3390/catal7030088.

[36] S. Wang, R.J. Farrauto, S. Karp, J.H. Jeon, E.T. Schrunk, Parametric, cyclic aging and characterization studies for CO_2 capture from flue gas and catalytic conversion to synthetic natural gas using a dual functional material (DFM), J. CO_2 Util. 27 (2018) 390–397, https://doi.org/10.1016/j.jcou.2018.08.012.

[37] A. Porta, R. Matarrese, C.G. Visconti, L. Lietti, Investigation of DFMs for CO_2 capture and methanation by coupled microreactor experiments and FT-IR spectroscopy, Energy Fuels (2023), https://doi.org/10.1021/acs.energyfuels.3c00443.

[38] S. Wang. A Study of Carbon Dioxide Capture and Catalytic Conversion to Methane using a Ruthenium, "Sodium Oxide" Dual Functional Material: Development, Performance and Characterizations, Ph.D., Columbia University, 2018.

[39] National Academies of Sciences, Engineering, and Medicine, Negative Emissions Technologies and Reliable Sequestration: A Research Agenda, The National Academies Press,, Washington, D.C., 2019.

[40] M.J. Realff, P. Eisenberger, Flawed analysis of the possibility of air capture, E1589–E1589, Proc. Natl. Acad. Sci. 109 (2012), https://doi.org/10.1073/pnas.1203618109.

[41] R.M. Heck, S. Gulati, R.J. Farrauto, The application of monoliths for gas phase catalytic reactions, Chem. Eng. J. 82 (2001) 149–156, https://doi.org/10.1016/S1385-8947(00)00365-X.

[42] M. Abdallah, R. Farrauto, A perspective on bridging academic research and advanced testing on a path towards pilot plant implementation: a case study of integrating CO_2 capture and catalytic conversion with dual function materials, Catal. Today (2022), https://doi.org/10.1016/j.cattod.2022.10.005.

[43] X. Gao, Z. Wang, Q. Huang, M. Jiang, S. Askari, N. Dewangan, S. Kawi, State-of-art modifications of heterogeneous catalysts for CO_2 methanation – active sites, surface basicity and oxygen defects, Catal. Today 402 (2022) 88–103, https://doi.org/10.1016/j.cattod.2022.03.017.